Nieto-Cerezo, O., and J. M. F. Mendoza. 2026. "Circularity Governance Under Strategic Incentives: A Stackelberg Model of Wind Turbine Blade Recycling." *Business Strategy and the Environment* 1–18.

which has been published in final form at

https://doi.org/10.1002/bse.70717.

Circularity Governance under Strategic Incentives: A Stackelberg Model of Wind Turbine Blade Recycling

Oscar Nieto-Cerezo[a,*], Joan Manuel F. Mendoza[a,b]

[a] *Mondragon University, Faculty of Engineering, Department of Mechanical and Industrial Production, Loramendi 4, 20500 Arrasate–Mondragon, Spain*
[b] *Ikerbasque, Basque Foundation for Science, Plaza Euskadi 5, 48009 Bilbao, Bizkaia, Spain*

Abstract

Circular economy goals under the European Green Deal require business models that make recyclability financially attractive, yet this alignment becomes fragile when eco-design effort is hidden and secondary-market prices are volatile. This paper develops a formal model of the wind-turbine blade (WTB) value chain to examine when closed-loop systems can internalise eco-design incentives. In a Stackelberg game between a manufacturer and a recycler, we show that reintegrating recovered Glass Fiber Reinforced Polimer (GFRP) into new WTBs can endogenously reward eco-design by linking material recovery to cost savings. However, this self-alignment weakens under risk aversion and competitive leakage, when recyclers divert material to more profitable external markets. We derive a robustness-adjusted subsidy threshold that ensures closed-loop stability and quantify how it varies with eco-design leverage, price uncertainty, and technology choice. Numerical results for pyrolysis and solvolysis highlight how technological maturity and market risk shape feasibility.

Keywords: Circular Governance, Closed-Loop Recycling,

*Corresponding author

Email addresses: onieto@mondragon.edu (Oscar Nieto-Cerezo), jmfernandez@mondragon.edu (Joan Manuel F. Mendoza)

Performance-Based Subsidies, Game Theory, Leakage Risk, Sustainability Strategy

---

1. Introduction

The transition to a circular economy is widely recognised as essential for reducing resource dependence, carbon emissions and waste generation. Yet in practice, circularity frequently falls short of policy ambitions, as structural frictions, behavioural responses and market uncertainties undermine recycling and eco-design measures (Korhonen et al., 2018; Stahel, 2016). These implementation gaps highlight a broader issue of circular governance: how to structure institutions, incentives and coordination mechanisms that align firm behaviour with circular outcomes under real-world constraints.

WTBs are a critical test case. They are large, composite-intensive products with rapidly growing end-of-life (EoL) volumes but limited high-value recycling pathways. Despite EU targets to eliminate blade landfill by 2025 (European Commission, 2020b, 2019) and industry pledges of "fully recyclable" blades (Siemens Gamesa Renewable Energy, 2021; Vestas Wind Systems A/S, 2023), most decommissioned WTBs continue to be used in low-value applications such as cement co-processing (Rosa et al., 2021; Beauson, 2022; Sproul et al., 2023). The competitiveness gap between virgin and secondary composites remains substantial. Although voluntary take-back schemes and design-for-recyclability initiatives have expanded under the EU Circular Economy Action Plan (WindEurope, 2020), large-scale closed-loop recycling remains rare. This persistent gap between ambition and outcomes suggests that technological advances alone are insufficient: economic, behavioural and institutional frictions continue to constrain circular transitions.

Subsidies for eco-design and recycling are among the most widely used instruments to support circularity. Cost-based subsidies offset processing costs but offer weak incentives for innovation, whereas performance-based schemes reward realised circular outcomes (Yu et al., 2021; Zhao et al., 2024). Yet even performance-based subsidies face major challenges. Eco-design effort is difficult to observe, creating scope for greenwashing and subsidy misallocation. High-profile announcements of "fully recyclable" blades often overstate actual progress, with most EoL composites still routed to cement kilns (Beauson, 2022; Sproul et al., 2023; WindEurope, 2023). These dynamics illustrate that circular transitions are fundamentally shaped by firms' strategic behaviour under sustainability constraints, because incentives and information asymmetries ultimately determine whether circular practices materialise in practice. Beyond informational asymmetry, market volatility, risk aversion and diversion of recovered GFRP to higher-value external markets further weaken policy effectiveness. Similar issues arise in renewable energy support, carbon offset markets and biofuel mandates, where unverifiable claims and weak monitoring have enabled rent-seeking and overstated environmental performance (Altenburg and Engelmeier, 2013; Calel et al., 2025; de Gorter et al., 2013). Extended producer responsibility (EPR) systems show comparable gaps between reported and actual recycling rates (OECD, 2016). Collectively, this evidence underscores how informational asymmetries and risk imbalances shape circular economy performance.

A growing literature highlights that circular transitions are hindered by market failures, misaligned incentives and coordination problems along value chains. Firms often struggle to reconcile environmental and economic objectives, and circular practices fail to scale when cooperation is weak or value distribution is uncertain (Enciso-Alfaro and García-Sánchez, 2025; Boukhatmi and Van Opstal, 2025). At the firm level, circular investments depend critically on decision-making under uncertainty, as volatility in material prices, technology performance, and regulatory signals shapes how companies balance environmental and economic objectives. Recent reviews show that theoretical advances remain fragmented, with the field lacking analytical frameworks that explain strategic behaviour, incentive formation and governance mechanisms in circular systems (Aryee, 2025). While game-theoretic and optimisation approaches have shed light on cooperation in industrial symbiosis (Yazan et al., 2020), coordination in re-commerce systems (Agrawal et al., 2023) and incentive-based product recovery (Gautam and Bolia, 2024), this work primarily addresses operational or bilateral pricing issues. It does not consider deeper governance challenges such as hidden effort, strategic underinvestment or competitive leakage. Analytical models of policy incentives in recycling remain limited. For instance, Bimonte et al. (2022) analyse eco-innovation support using a Stackelberg framework but do not capture eco-design effort or closed-loop coordination, while work on digital platforms addresses market failures (Boukhatmi and Van Opstal, 2025) without modelling vertical governance in manufacturing.

As a result, there is still no analytical framework that integrates hidden eco-design effort, endogenous recycling decisions, performance-based subsidies, uncertainty and leakage into a unified model of closed-loop governance. This gap limits our understanding of when circular systems become self-enforcing and when policy intervention is required to stabilise them.

This paper addresses this gap by developing a governance-oriented analytical framework that treats circularity as a strategic coordination problem between manufacturers and recyclers. By linking governance design with circular business model strategy, the framework shows how institutional arrangements and incentive structures jointly determine the viability and stability of closed-loop systems.

The recycling value chain is represented as a Stackelberg game in which the manufacturer chooses the eco-design effort and the buy-back price, anticipating the recycler's optimal response. Eco-design effort is modelled as hidden from the policymaker, capturing a key governance friction, but remains observable to the recycler within the bilateral exchange. To examine how incentives can be realigned under real-world conditions, we introduce a performance-based subsidy that rewards realised circular outcomes and analyse its effectiveness under volatility, risk aversion, and competitive leakage. The model formalises how closed-loop systems can endogenously reward eco-design, and how this alignment weakens when recyclers divert materials to external markets or when uncertainty discourages investment.

The analysis yields several implications for circular economy governance and business strategy. A key result is the identification of a robustness-adjusted subsidy threshold that determines whether circular systems can be sustained without additional intervention. This threshold increases with technological volatility, eco-design leverage and material-retention requirements, suggesting that static subsidy levels may be insufficient under risk. These results inform the design of performance-based policies and highlight the need for complementary instruments, such as procurement commitments, monitoring systems and traceability, that reduce information asymmetries and limit leakage. For firms, the model offers strategic insight into how contractual arrangements and risk-sharing schemes can stabilise circular partnerships under uncertainty.

Building on these implications, this paper makes three strategic contributions to the literature on circular economy governance and business strategy.

First, it conceptualises circularity not simply as a technological or operational challenge, but as a strategic coordination problem between manufacturers and recyclers operating under hidden eco-design effort, uncertainty and competing market opportunities. By framing circularity as an incentive-alignment issue, the analysis highlights why circular systems that appear viable on paper often fail to stabilise in practice. Second, the paper characterises the conditions under which closed-loop systems become endogenously self-governing, that is, capable of sustaining eco-design and material retention through internal cost-saving feedbacks, versus those under which they remain dependent on policy support, particularly when firms are risk-averse or when leakage to external markets is profitable. Third, the paper introduces a robustness-adjusted subsidy threshold that links performance-based policy design to technological characteristics, market volatility and leakage risk, offering a governance-relevant metric for assessing when subsidies alone are sufficient and when complementary instruments are required.

While the model is calibrated to WTBs recycling, the underlying mechanisms apply to a broad class of circular value chains, such as composite-intensive manufacturing, electronics and construction materials, where eco-design effort is difficult to observe, secondary markets are volatile, and long-term circular coordination is strategically fragile.

2. Analytical Framework

This section presents an analytical framework to study circular governance in the WTB value chain. The model considers two strategic actors, a manufacturer and a recycler, engaged in a closed-loop relationship. Rather than constructing a fully specified principal–agent contract, the model focuses on characterising the strategic interdependence between manufacturers and recyclers and on assessing how governance mechanisms can support circular performance. The interaction is represented as a Stackelberg game in which the manufacturer, acting as leader, chooses an unobservable eco-design effort and a buy-back price, anticipating the recycler's optimal response. The recycler observes these choices and decides the recycling rate, which determines the share of EoL material reintegrated into the production of new WTBs (see Figure 1).

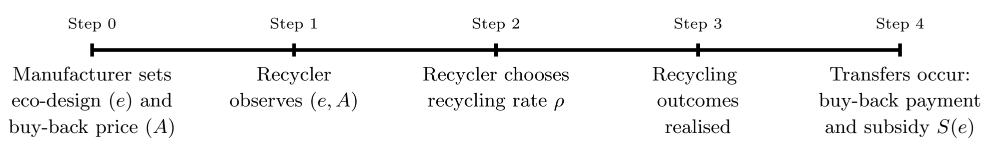

Figure 1: Decision timeline in the Stackelberg model: the manufacturer (leader) chooses eco-design effort and the buy-back price, anticipating the recycler's (follower) recycling decision.

This structure reflects industry practice, i.e., design standards are determined ex ante, while recycling decisions are made ex post, and captures institutional asymmetries in information and control. It also operationalises an ecological economics perspective by examining how circularity emerges endogenously under imperfect monitoring rather than assuming perfect enforcement. Model outcomes include eco-design effort, recycling rates, firm payoffs, and the subsidy level required to sustain full material retention in the closed-loop system.

Government support for eco-design is modelled as a linear performance-based subsidy, reflecting performance-based policy schemes that reward realised circular outcomes while remaining simple and transparent

$$S(e) = \delta e q, \tag{1}$$

where $e \geq 0$ denotes eco-design effort, $\delta > 0$ the subsidy rate, and $q > 0$ the number of WTBs manufactured in the period[1]. Linear performance-based schemes are consistent with emerging extended producer responsibility (EPR) principles and reflect current EU momentum toward linking design choices to EoL outcomes (WindEurope, 2020; OECD, 2016; European Commission, 2008).

Figure 2 situates the model within the WTB value chain, illustrating the material flows, strategic decisions and informational frictions that motivate the analytical structure.

Eco-design effort e captures increasingly complex design modifications, such as modular interfaces, reversible adhesives and traceable components (Sardana et al., 2024; Martinez Leal et al., 2020). While higher effort raises

[1] In a closed-loop context, q also represents the number of WTBs re-entering the system at end-of-life.

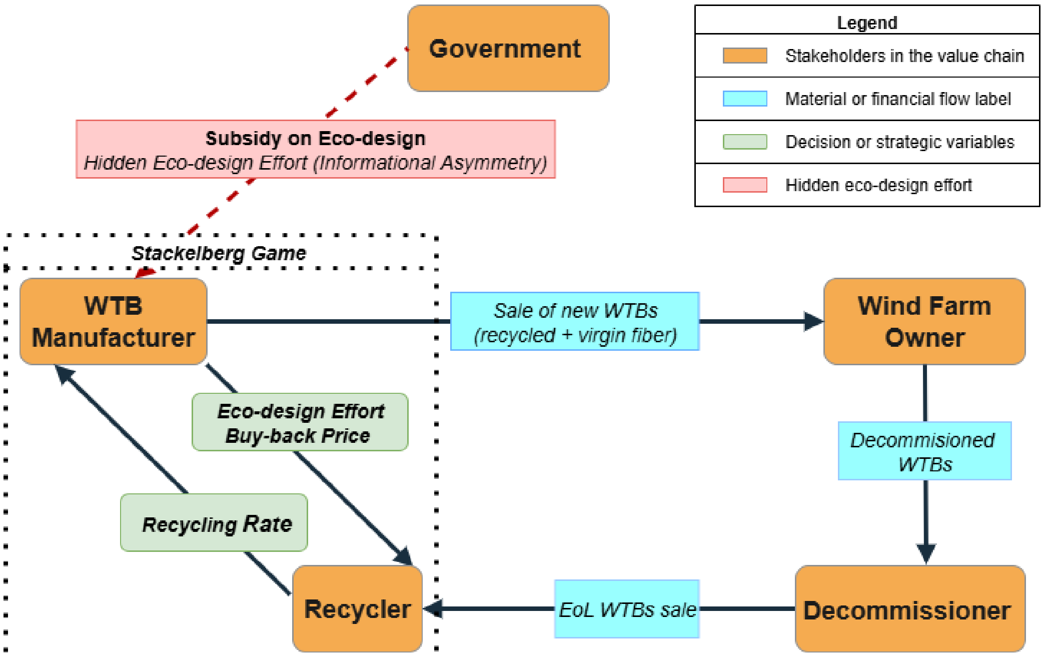

Figure 2: Structure of the WTB recycling value chain showing the Stackelberg interaction between the manufacturer and recycler under hidden eco-design effort and informational asymmetry.

manufacturing costs, it also enhances the quality and recovery of composite materials at EoL. The manufacturer also sets a buy-back price A, interpreted as a per-ton payment to the recycler to secure the return of recovered fibres and prevent diversion to external markets, thereby enabling their reintegration into the production of new WTBs (Sproul et al., 2023; Pender et al., 2024). The recycler responds by choosing a recycling rate $\rho \in [0, 1]$, determining the fraction of composite material returned to the closed-loop system. As ρ approaches full circularity, marginal recycling costs rise due to contamination limits, sorting complexity and diminishing-quality fractions. Decommissioners and asset owners, while not modelled as strategic actors, influence material flows through dismantling and transport decisions. Their role forms part of the institutional infrastructure that shapes the effectiveness of closed-loop recycling systems (Ferrell and DeVuyst, 2013; Beauson, 2022).

Eco-design incurs a quadratic cost:

$$\psi(e) = \frac{de^2}{2}, \tag{2}$$

reflecting increasing marginal costs of design improvements as more advanced eco-design features, e.g. modular architectures, reversible bonding, or traceability requirements, are implemented. At EoL, higher eco-design effort increases the mechanical performance of recovered fibres to $h_{ts}+\lambda e$, where h_{ts} is the baseline tensile strength and λ captures the marginal effect of eco-design effort on material tensile strength. Tensile strength is the key mechanical property determining whether recycled composite fibres can be reintegrated into structural WTB production rather than downcycled[2]

The manufacturer's revenue is therefore:

$$\tilde{\pi}(e) = \tilde{\beta}(h_{ts} + \lambda e)q, \tag{3}$$

where $\tilde{\beta}$ is a stochastic price capturing fluctuations in demand, raw material costs and policy uncertainty (McKinsey & Company, 2023; Rahman and Shakeel, 2025; Thapa and Missoum, 2022).

Recycling is economically attractive only when the closed-loop value of

[2]Tensile strength measures the maximum stress a fibre can withstand before failure. Higher tensile strength increases the likelihood that recovered fibres meet structural performance thresholds for WTB manufacturing (Tapper et al., 2018).

recycled material exceeds the buy-back price:

$$\Delta > A,$$

where Δ denotes the per-unit closed-loop value associated with reintegrating recycled material into production [3]. Net savings are:

$$R(A) = (\Delta - A)\,\mathcal{M}\,\rho\,q\,v, \tag{4}$$

where $\mathcal{M}$ is the GFRP content per blade and v denotes blade mass.

The manufacturer's payoff is given by:

$$P(e, A) = \tilde{\pi}(e) + S(e) + R(A) - \psi(e), \tag{5}$$

combining revenue, subsidy income, cost savings and eco-design costs.

The recycler's gross profit from material recovery is:

$$\Pi(\rho) = (A - B - C_{rm} + \theta e)\,\mathcal{M}\rho q v, \tag{6}$$

where B captures upstream decommissioning costs associated with WTB disassembly and cutting, C_{rm} denotes the recycler-side per-unit recycling cost, including transport and the recycling process (e.g., pyrolysis or solvolysis), and θe represents the per-unit cost reduction induced by eco-design effort. [4]

Increasing the recycling rate imposes rising marginal costs:

$$\varphi(\rho) = \frac{k\rho^2}{2}, \tag{7}$$

[3] This value reflects, among other components, avoided energy use and raw material extraction relative to virgin GFRP (Oliveux et al., 2015).

[4] Eco-design can reduce chemical inputs, energy demand and process complexity. For example, through reversible adhesives or modular interfaces (Oliveux et al., 2015).

reflecting economic limits to full circularity. Recycling costs are assumed to be convex in the recovery rate, capturing increasing marginal costs associated with higher material recovery, such as quality losses, processing complexity, and capacity constraints. The recycler's net payoff is:

$$P_r(\rho) = \Pi(\rho) - \varphi(\rho). \tag{8}$$

These payoff functions allow us to examine how informational, behavioural and structural frictions shape circularity outcomes. While the model is calibrated to the WTB recycling context, several elements of the framework are not specific to this application. In particular, the treatment of eco-design as a hidden effort, the use of performance-based subsidies, the role of price uncertainty and risk aversion, and the possibility of leakage to alternative markets capture governance challenges that are common to a wide range of circular value chains. By contrast, the specific parameter values, cost structures, and recycling technologies considered in the numerical analysis reflect characteristics of the WTB sector.

To assess how circularity behaves under increasing real-world complexity, we extend the model in three stages, illustrated in Figure 3.

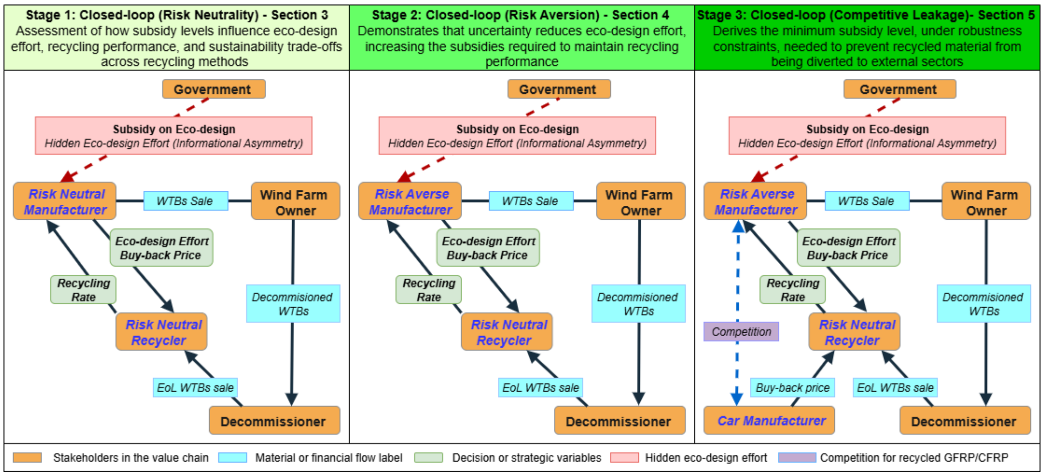

Figure 3: Model extensions: (1) risk-neutral closed loop, (2) risk-averse closed loop, and (3) closed loop with competitive leakage.

We begin with a benchmark risk-neutral closed loop without leakage. This provides closed-form solutions for eco-design and recycling under ideal alignment. We then incorporate manufacturer risk aversion under stochastic WTB prices, reflecting real exposure to market volatility and policy uncertainty. Risk reduces eco-design effort and increases the subsidy required to sustain circularity. Finally, we introduce competitive leakage, allowing recyclers to divert recovered fibres to external markets. This extension captures systemic challenges associated with open material flows and enables the derivation of a robustness-adjusted subsidy threshold required to retain material within the WTB value chain.

Together, these stages align ecological economics insights on bounded rationality, uncertainty and leakage with firm-level incentives and circularity targets, illustrating when circularity can be self-enforcing and when complementary policy intervention becomes necessary.

3. Risk-Neutral Closed-Loop Benchmark

We begin with a benchmark case in which both manufacturer and recycler are risk-neutral and all recovered material is fully reintegrated into new WTBs, with no leakage to external sectors. Although uncertainty is present through market volatility in blade prices, risk-neutral agents maximize expected profits and are unaffected by variance. In our Stackelberg game framework, the strategic interaction between the manufacturer and the recycler unfolds in two stages. The manufacturer, as the leader, first sets the eco-design level (e) and the buy-back price (A). The recycler, as the follower, then determines the optimal recycling rate (ρ) in response. The game is solved by backward induction, starting from the recycler's decision and moving backward to the WTB manufacturer's decision, ensuring that both parties' strategies are optimized given the sequential nature of the interaction.

Throughout this section, hidden effort refers, as in Section 2, to the incentive misalignment that arises when the manufacturer's eco-design effort is unobservable to the policymaker.

We measure system-level circularity through the recycling rate (ρ). Full circularity ($\rho = 1$) means that 100% of recovered GFRP is reintegrated into new WTBs by the original manufacturer. This outcome corresponds to the industry-led ambitions for "full blade recyclability" and the elimination of landfill disposal under circular economy roadmaps (European Commission, 2020b, 2019; WindEurope, 2020). Partial circularity ($\rho < 1$) occurs when only part of the recovered material returns to blade production due to technical limits or prohibitive marginal costs.

We now turn to the recycler's decision problem. Substituting Eq. 6 and Eq. 7 into Eq. 8, the recycler's pay-off becomes:

$$P_r(\rho) = (A - B - C_{rm} + \theta e)\, vq\mathcal{M}\, \rho \;-\; \frac{k}{2}\rho^2. \tag{9}$$

where B denotes the decommissioning payment paid to the decommissioner, and C_{rm} denotes the recycler-side per-unit recycling cost, θe represents the per-unit cost reduction induced by eco-design effort, v the WTB mass, q the number of decommissioned blades, and $\mathcal{M}$ the GFRP content per WTB. Formally, the optimization problem reads

$$\max_{0 \le \rho \le 1} P_r(\rho). \tag{10}$$

Lemma 1. *The recycler's decision problem has a unique interior solution ρ^*, which is determined by the first-order condition (FOC)*

$$k\rho^* = (A - B - C_{rm} + \theta e) vq\mathcal{M}. \tag{11}$$

Moreover, the optimal recycling rate $\rho^* = \rho^*(e, A)$ is strictly increasing in both e and A.

Proof. The proof of Lemma 1 is provided in the Appendix.

Lemma 1 indicates that stronger buy-back commitments by manufacturers and higher eco-design effort directly incentivize recyclers to raise recovery rates, thereby reinforcing the closed-loop structure.

Substituting the expressions for revenue, subsidy income, recycling savings, and eco-design costs into the WTB manufacturer's payoff, and using the recycler's best response $\rho^*(e, A)$, the manufacturer's payoff can be written as

$$\tilde{P}(e,A) = \tilde{\beta}(h_{ts} + \lambda e)q + \delta eq + (\Delta - A)\rho^* qv\mathcal{M} - \frac{d}{2}e^2 \tag{12}$$

For consistency, we refer to $\tilde{P}(e,A)$ as the WTB manufacturer's stochastic payoff, and under risk neutrality we maximise its expected value.

The distribution of the unit revenue coefficient can be approximated by a log-normal PDF, $\tilde{\beta} \sim \mathrm{LN}(\mu_\beta, \sigma_\beta^2)$, because it ensures positive prices, reflects right skewed market price fluctuation, and accounts for multiplicative economic uncertainty [5].

$$f(\beta) = \frac{1}{\beta\sqrt{2\pi\sigma_\beta^2}} \exp\left(-\frac{(\ln\beta - \mu_\beta)^2}{2\sigma_\beta^2}\right), \quad \beta > 0 \tag{13}$$

Replacing ρ^* by the FOC in Eq. 11 and $f(\beta)$ by the log-normal PDF in Eq. 13, the expected profit of the WTB manufacturer takes the form:

$$\begin{aligned}\mathbb{E}[\tilde{P}(e,A)] = \int_0^\infty \Bigg[&\beta(h_{ts} + \lambda e)q + \delta eq \\ &+ \frac{(\Delta - A)(A - B - C_{rm} + \theta e)v^2 q^2 \mathcal{M}^2}{k} - \frac{d}{2}e^2\Bigg] f(\beta)\, d\beta\end{aligned} \tag{14}$$

Since $f(\beta)$ is the PDF of β, the expectation only affects terms containing β. Under the log-normal distribution, $\mathbb{E}[\beta] = \exp\left(\mu_\beta + \frac{\sigma_\beta^2}{2}\right)$, so the first term

[5] The price of recycled WTBs is influenced by multiple factors following a normal distribution, whose product results in a lognormal price distribution (Fonte and Xydis, 2021). Due to the underdeveloped market and uncertain demand, prices exhibit high variability and skewness (Chen et al., 2019).

in the profit expression is obtained by replacing β with this mean value.

$$\begin{aligned}\mathbb{E}[\tilde{P}(e,A)] =& exp(\mu_\beta + \frac{\sigma_\beta^2}{2})(h_{ts} + \lambda e)q + \delta eq \\ &+ \frac{(\Delta - A)(A - B - C_{rm} + \theta e)v^2 q^2 \mathcal{M}^2}{k} - \frac{d}{2}e^2\end{aligned} \tag{15}$$

Anticipating the recycler's optimal response (ρ^*), the WTB manufacturer strategically chooses the levels of eco-design (e), and the buy-back price (A). These decisions are chosen to maximize the WTB manufacturer's expected payoff.

$$\max_{e,A} \mathbb{E}[\tilde{P}(e,A)] \tag{16}$$

Lemma 2. *The manufacturer's optimal decisions for eco-design effort e^* and buy-back price A^* are characterized by the FOC:*

$$dke^* = qv\left[\mathcal{M}^2 qv\theta\,(\Delta - A^*) + k\left(\delta + \lambda\exp\left(\mu_\beta + \frac{\sigma_\beta^2}{2}\right)\right)\right] \tag{17}$$

$$2A^* = \Delta + B + C_{rm} - \theta e^* \tag{18}$$

Equation 17 shows that e^* rises with the subsidy rate δ, the tensile-strength gain from eco-design λ, and the profitability of recycling $(\Delta - A^*)$. Equation 18 shows that, as eco-design improves, the manufacturer can offer a lower buy-back price and still make recycling attractive for the recycler, since better design reduces the recycler's effective costs.

Proof. The proof of Lemma 2 is provided in the Appendix.

Lemma 2 shows that subsidies, technological improvements in GFRP quality, and the profitability of recycled versus virgin material are the key levers that stimulate eco-design

Combining Lemmas 1 and 2, we derive the unique closed-loop equilibrium for the risk-neutral benchmark model:

Proposition 1. *The unique closed-loop equilibrium in the risk-neutral case is determined by the following:*

1. *The optimal buy-back price is:*

$$A^{**} = \frac{dk(\Delta + B + C_{rm}) - \theta qv \left(\mathcal{M}^2 qv\theta\Delta + k(\delta + \lambda \exp(\mu_\beta + \frac{\sigma_\beta^2}{2})) \right)}{2dk - \mathcal{M}^2 q^2 v^2 \theta^2} \tag{19}$$

2. *The optimal eco-design level is:*

$$e^{**} = \frac{2qvk \left(\frac{\mathcal{M}^2 qv\theta}{2k} (\Delta - B - C_{rm}) + \delta + \lambda \exp(\mu_\beta + \frac{\sigma_\beta^2}{2}) \right)}{2dk - \mathcal{M}^2 q^2 v^2 \theta^2} \tag{20}$$

3. *The corresponding recycling rate implemented by the recycler is:*

$$\rho^{**} = \frac{(A^{**} - B - C_{rm} + \theta e^{**}) vq\mathcal{M}}{k} \tag{21}$$

While the interior equilibrium is analytically tractable, whether the boundary outcome $\rho = 1$ (full circularity) is attained depends on nonlinear parameter interactions that cannot be resolved analytically. Because $\rho = 1$ corresponds to EU circularity targets, we use numerical simulations to examine the subsidy levels required to sustain full circularity and assess whether such thresholds are economically and politically feasible.

3.1. Subsidy Requirements and Strategic Trade-Offs Under Risk-Neutral Circularity

3.1.1. Recycling Technologies and Data Inputs

The analysis compares two representative recycling methods, pyrolysis (M1) and solvolysis (M2), that differ in technological maturity, cost structure, recovery efficiency, and achievable GFRP quality. Table 1 summarises their key characteristics.

Table 1: Summary of recycling methods for EoL WTBs.

Method	**Process Description**	**Main Outputs**	**Reference**
M1	Thermal decomposition in the absence of oxygen, breaking down composite materials into hydrocarbon-based compounds.	Fibres, oil, gas, carbon black	Szatkowski and Twaróg (2024)
M2	Chemical recycling using solvents to dissolve the polymer matrix and recover fibres with high mechanical integrity.	Fibres, oil	Lund and Madsen (2024)

To operationalise the analytical framework developed in Section 3, we calibrate parameters using recent techno-economic data for EoL WTBs. Table 2 summarises the main model parameters, their economic interpretation, units, baseline values for pyrolysis and solvolysis, and data sources.

We adopt a representative 48.7 m blade from a 1.7 MW turbine (Sproul et al., 2023), with total mass $v = 9\,\text{t}$, of which $\mathcal{M} = 0.587$ is GFRP. The decommissioning payment $B = 64.1\,€/\text{t}$ represents disassembly and cutting, while recycler-specific processing costs combine transport and recycling com-

[6] Decommissioning payment (B) aggregates disassembly and cutting costs reported in Table 3 of Liu et al. (2022).

[7] Recycler-side recycling costs (C_{rm}) aggregate transport and process-level recycling costs reported in the same source.

Table 2: Model parameters, units, baseline values, and data origin.

Symbol	Description	Unit	(M1)	(M2)
B	Decommissioning payment*[6]	€/t	64.1	64.1
C_{rm}	Recycler-side recycling cost*[7]	€/t	304.0	779.3
ρ_0	Baseline recycling rate*	–	0.75	0.85
h_{ts}	Baseline tensile strength*	GPa	1.2	2.0
θ	Eco-design leverage†	€/t	13.82	13.82
λ	Tensile-strength gain from eco-design†	GPa	0.01	0.01
Δ	Closed-loop material value‡	€/t	4500	4500
d_0	Eco-design cost scale†	–	37	37
k	Recycling cost curvature†	–	310000	26000
μ_β	Log-mean revenue coefficient‡	–	9	9
σ_β	Revenue volatility‡	–	1.0	1.0

Note: * Empirical parameters sourced from the literature cited in the manuscript; † calibrated parameters chosen to match observed techno-economic characteristics of the recycling technologies; and ‡ assumed parameters used for scenario analysis.

ponents from Table 3, yielding $C_{rm,M1} = 304.0$ €/t and $C_{rm,M2} = 779.3$ €/t. Secondary-market uncertainty is captured by a lognormal unit-revenue coefficient, $\ln \beta \sim \mathcal{N}(9, 1.0^2)$, consistent with Eq. 13.

Baseline performance parameters reflect the existing technical capabilities of each recycling method,[8] as documented in reported recovery yields and

[8] Here, “baseline” refers to the method-specific recovery performance observed in laboratory and pilot-scale trials before any eco-design effort by the manufacturer. Thus,

Table 3: Breakdown of process-level recycling costs for EoL WTB (€/t), adapted from Liu et al. (2022).

	Disassembly (€/t)	Cutting (€/t)	Transport (€/t)	Recycling (€/t)	Total (€/t)
M1: Pyrolysis	25.9	38.2	96.7	207.3	364.9
M2: Solvolysis	25.9	38.2	96.7	682.6	843.3

tensile–strength retention studies. Pyrolysis typically achieves 70–80% recovery, with fibres retaining 60–70% of their original tensile strength (approximately 1.1–1.4 GPa) (Giorgini et al., 2016; Åkesson et al., 2012). Solvolysis performs better, reaching 85–90% recovery efficiency and producing fibres with strength close to virgin composites. Because absolute strength values are not consistently reported, we adopt a conservative recovered-strength benchmark of 2.0 GPa, consistent with upper-bound experimental estimates (Zabihi et al., 2020; Sokoli et al., 2017) and corresponding to the minimum tensile-strength level typically required for structural-grade reuse in new WTB manufacturing.[9]

These considerations motivate the baseline parameter values $\rho_{0,M1} = 0.75$, $h_{ts,M1} = 1.2\,\text{GPa}$, $\rho_{0,M2} = 0.85$, and $h_{ts,M2} = 2.0\,\text{GPa}$. To ensure consistency between empirical performance and model structure, these baseline values

$\rho_{0,M1} = 0.75$ and $\rho_{0,M2} = 0.85$ represent current achievable recovery levels, not a zero-recovery starting point.

[9]Industry and laboratory evidence indicate that tensile strengths around 2.0 GPa represent the lower bound for structural composite applications, including new wind turbine blades.

ρ_{0,M_i} also define the reference recovery levels in the recycling cost function introduced below, representing the minimum-cost operating points for each technology.

Parameters governing incentive responsiveness, including eco-design leverage ($\theta = 13.82$), the tensile-strength gain from eco-design ($\lambda = 0.01$), and the closed-loop material value ($\Delta = 4500$ €/t), are held constant across methods. These values are not directly estimated from data but are chosen to produce realistic equilibrium behaviour: moderate improvements from eco-design, diminishing marginal returns, and buy-back prices aligned with European GFRP markets. Together, they balance empirical grounding with internal model consistency, making the numerical analysis interpretable for academic and policy audiences.

Eco-design effort is represented by the quadratic cost function

$$\psi(e) = \frac{d_{M_i}}{2}\, e^2, \qquad d_{M_i} = \frac{d_0}{(1-\rho_{0,M_i})^{\eta}}, \quad d_0 = 37,\ \eta = 1.2.$$

Higher baseline recovery rates yield steeper cost curves, reflecting the increasing marginal difficulty of design improvements as circularity approaches its technical limits (Bocken et al., 2014). The calibrated coefficients are $d_{M1} = 21{,}756$ and $d_{M2} = 25{,}679$.

Recycler costs are modelled as

$$\varphi_{M_i}(\rho) = \frac{k_{M_i}}{2}(\rho^2 - \rho_{0,M_i}^2) + \kappa_{M_i}\, \frac{(\rho - \rho_{0,M_i})_+^2}{(1-\rho_{0,M_i})^{\xi_{M_i}}}, \tag{22}$$

where k_{M_i} captures baseline curvature, κ_{M_i} determines the penalty magnitude, and ξ_{M_i} controls the steepness of cost escalation near the recovery frontier. In the numerical analysis, we replace the benchmark quadratic cost $\varphi(\rho) = \frac{k}{2}\rho^2$ used in the analytical sections with the method-specific calibrated function $\varphi_{M_i}(\rho)$ in Eq. 22 to capture observed nonlinear cost escalation as recovery approaches its technological limit.

The parameter values are $k_{M1} = 310{,}000$, $\kappa_{M1} = 57$, $\xi_{M1} = 0.1$ for pyrolysis, and $k_{M2} = 26{,}000$, $\kappa_{M2} = 250$, $\xi_{M2} = 2.7$ for solvolysis. This specification ensures $\varphi_{M_i}(\rho_{0,M_i}) = 0$ [10]

Figure 4 visualises the calibrated eco-design and recycling cost functions. In Panel (a), higher η steepens $\psi_{M_i}(e)$, illustrating the growing marginal difficulty of design improvements. In Panel (b), higher ξ_{M_i} sharpens the escalation in $\varphi_{M_i}(\rho)$ near $\rho = 1$, capturing the nonlinear cost increase associated with approaching full recovery.

(a) Eco-design cost functions.

(b) Recycling cost functions.

Figure 4: Calibrated cost functions for the two recycling methods. Dashed lines mark baseline recovery rates $\rho_{0,M1} = 0.75$ and $\rho_{0,M2} = 0.85$.

These calibrated relationships show that as circularity approaches its technical limits, marginal costs rise sharply. The subsequent analysis examines how subsidy levels interact with these nonlinearities to determine whether closed-loop outcomes remain economically viable.

[10] For numerical optimisation, the non-differentiable operator $(\rho - \rho_0)_+$ is approximated by

$$(\rho - \rho_0)_+ \approx \frac{1}{2}\left[(\rho - \rho_0) + \sqrt{(\rho - \rho_0)^2 + \epsilon^2}\right], \qquad \epsilon = 10^{-10},$$

which preserves the original functional shape while ensuring smooth derivatives.

3.1.2. Results: Circularity Outcomes and Strategic Insights

Numerical calculations were performed using Python (SciPy 1.14). The recycler's best response for ρ admits a closed-form solution, while the manufacturer's bi-level problem in (e, A) was solved via nonlinear programming (SLSQP). Results were validated against a grid search over (e, A) to check for consistency and rule out obvious local optima. Subsidy scenarios were simulated for $\delta = \{0, 250, 500, 750\}$ and extended iteratively until $\delta_{M_i}^{100\%}$, the minimum subsidy achieving full circularity ($\rho_{M_i}^{**} = 1$), was identified. Table 4 summarises the equilibrium values of eco-design effort ($e_{M_i}^{**}$), buy-back price ($A_{M_i}^{**}$), and recycling rate ($\rho_{M_i}^{**}$) for both recycling methods across increasing subsidy levels.

Table 4 shows that subsidies increase eco-design effort and recycling rates nonlinearly: modest support yields rapid gains, but approaching $\rho = 1$ requires disproportionately large transfers. As δ rises, $(e_{M_i}^{**}, A_{M_i}^{**}, \rho_{M_i}^{**})$ move jointly toward full closed-loop, but the marginal subsidy grows steeply near the frontier, an instance of diminishing institutional returns. Beyond this point, additional fiscal effort yields smaller systemic gains and may threaten fiscal sustainability. Hence, subsidies alone cannot substitute for feedback mechanisms, such as design standards, traceability, and quality certification, that stabilize circular relationships.

Solvolysis (M2), while technologically superior, requires a higher subsidy coefficient $\delta_{M_i}^{100\%}$ to achieve full circularity than pyrolysis (M1). This difference stems from two structural factors: first, solvolysis has a steeper eco-design cost curve ($d_{M2} = 25{,}679$ vs. $d_{M1} = 21{,}756$), reflecting the increasing difficulty of design improvements near its higher baseline recovery rate; and

Table 4: Equilibrium decision variables and payoffs for different subsidy levels δ.

	Variable	$\delta = 0$	$\delta = 250$	$\delta = 500$	$\delta = 750$	$\delta_{M_i}^{100\%}$
	e_{M1}^{**}	19.3	45.4	71.4	97.5	125.0
	A_{M1}^{**} (€)	2785	2120	1940	1760	1565
M1	ρ_{M1}^{**} (%)	75.0	81.1	87.2	93.4	100.0
	Manufacturer Payoff (€)	510,025	671,610	963,505	1,385,711	1,988,059
	Recycler Payoff (€)	174,284	189,089	205,106	222,283	242,131
	e_{M2}^{**}	10.9	24.8	38.8	52.8	85.3
	A_{M2}^{**} (€)	2785	2663	2566	2470	2245
M2	ρ_{M2}^{**} (%)	85.0	87.2	90.1	93.1	100.0
	Manufacturer Payoff (€)	785,992	875,103	1,034,146	1,263,140	2,063,806
	Recycler Payoff (€)	187,850	194,291	203,351	212,706	235,601

$\delta_{M1}^{100\%} = 1020$; $\delta_{M2}^{100\%} = 1330$.

second, it faces higher recycling costs ($C_{rm,M2} = 779.3$ €/t vs. $C_{rm,M1} = 304.0$ €/t; Table 3). These factors raise the marginal fiscal effort required to stimulate additional eco-design investment, yielding $\delta_{M_2}^{100\%} = 1330$ compared to $\delta_{M_1}^{100\%} = 1020$. Yet because solvolysis attains circularity with lower effort ($e_{M2}^{**} = 85.3$ vs. $e_{M1}^{**} = 125$), the total subsidy outlay, $S_{M_i}^{**} = \delta_{M_i}^{100\%} e_{M_i}^{**} q$, is smaller; about €2.27 million for solvolysis versus €2.55 million for pyrolysis (for $q = 20$ blades). Hence, although solvolysis requires a higher per-unit subsidy, its technological efficiency reduces the overall fiscal burden of achieving full circularity.

Both agents benefit monotonically from increasing subsidies. Manufacturer payoffs grow faster because subsidies directly offset eco-design costs and raise the value captured from recycled fibres, while recycler gains expand more gradually through higher buy-back prices and reduced recovery costs. The widening gap between manufacturer and recycler payoffs reflects that most fiscal support accrues upstream, highlighting an equity dimension of subsidy design: without complementary sharing mechanisms, circularity gains may concentrate at the manufacturing tier rather than across the value chain.

The sensitivity of subsidy requirements to key parameters is summarised in Table 5. Entries report the percentage change in the minimum subsidy coefficient ($\delta_{M_i}^{100\%}$) needed to achieve full circularity when each parameter increases by 10%.

Two results stand out. First, ($\delta_{M_i}^{100\%}$) is most elastic to structural value drivers: a higher closed-loop material value (Δ) or stronger eco-design leverage (θ) substantially reduces the fiscal support required. Improvements in expected market conditions, captured by the revenue log-mean (μ_β), also lower subsidy needs.

Second, subsidy requirements increase with parameters that steepen the marginal cost of recovery or design effort. Higher recycling-cost curvature (k) or a steeper eco-design cost scale (d_0) significantly raise the subsidy threshold, as do higher recycler-side recycling costs (C_{rm}).

Taken together, these elasticities indicate that the most cost-effective levers for reducing fiscal support are those that raise intrinsic closed-loop value, i.e., higher Δ, stronger eco-design leverage θ, and more favourable price expectations μ_β. By contrast, steep cost-curvature parameters (k, d_0)

Table 5: Elasticity of the subsidy threshold ($\delta_{M_i}^{100\%}$) with respect to key parameters. Values indicate the % change in ($\delta_{M_i}^{100\%}$) resulting from a 10% increase in the parameter.

Parameter	M1: Pyrolysis (%)	M2: Solvolysis (%)
Δ (per-unit closed-loop value)	-30.9	-38.7
θ (Eco-design leverage)	-11.6	-11.3
C_{rm} (Recycler-side recycling cost)	$+2.45$	$+7.52$
μ_β (Log-mean of the revenue coefficient)	-19.1	-15.0
k (Recycler cost curvature)	$+41.7$	$+46.5$
d_0 (Eco-design cost scale)	$+11.9$	$+12.0$

rapidly increase subsidy requirements, highlighting the importance of process innovations and design improvements that flatten cost trajectories.

The numerical results allow the most sensitive parameters to be directly mapped to concrete managerial actions and policy instruments.Parameters with the largest impact on the subsidy threshold are those that increase the intrinsic value of closed-loop recycling. In particular, a higher closed-loop material value (Δ) corresponds to policy measures such as green public procurement, recycled-content requirements, or certification schemes that increase the effective market value of recycled GFRP relative to virgin materials.Similarly, stronger eco-design leverage (θ) reflects managerial and organisational investments that make design improvements more effective, such as design-for-recyclability choices, process integration, and information-sharing mechanisms that allow eco-design effort to translate more directly into lower downstream processing costs.By contrast, parameters that steepen cost trajectories, such as recycling cost curvature (k), eco-design cost scale (d_0), and recycler-side recycling costs (C_{rm}), capture technological immaturity and capacity constraints. These parameters point to the importance of technology support, learning-by-doing, and scale-up policies as complements to financial subsidies.

Closed-loop recycling becomes self-sustaining, i.e., achieves $\rho = 1$ without subsidies, only when the combined value of recycled materials and eco-design-induced cost savings is sufficiently high to offset rising marginal recovery costs. Moderate subsidies can trigger substantial improvements in recycling rates, but approaching full circularity requires disproportionately large fiscal support due to sharply increasing marginal costs. Technologies with higher baseline performance, such as solvolysis, reduce the total subsidy needed despite requiring higher per-unit support, highlighting the importance of technological efficiency rather than subsidy intensity alone as a key lever for both firms' design choices and policy targeting.

4. Risk-Averse Closed-Loop System

The analysis so far has assumed a risk-neutral manufacturer. We now relax this assumption by introducing risk aversion, capturing how uncertainty in secondary-material markets affects strategic choices in eco-design and recycling. In practice, manufacturers value stability in circular supply chains: volatile resale prices and uncertain fibre quality increase planning risks, influencing investment and contracting decisions. To model these strategic preferences, we adopt a constant absolute risk aversion (CARA) utility function which allows for a tractable representation of how uncertainty affects strategic decisions and policy thresholds.

The manufacturer's utility under uncertainty is:

$$u(\tilde{P}(e_u, A_u)) = -\exp\left\{-\gamma\left(\tilde{\beta}(h_{ts}+\lambda e_u)q + \delta e_u q + (\Delta - A_u)\rho^* \mathcal{M} q v - \frac{d}{2}e_u^2\right)\right\}, \tag{23}$$

where $\gamma > 0$ denotes the degree of risk aversion. The utility function is strictly increasing and concave, consistent with a preference for predictable circular value flows.

Expected utility becomes:

$$\begin{aligned} V(e_u, A_u) = -\exp&\left\{-\gamma\left(\delta e_u q + (\Delta - A_u)\rho^* \mathcal{M} q v - \frac{d}{2}e_u^2\right)\right\} \\ &\times \int_0^\infty \exp[-\gamma\beta(h_{ts}+\lambda e_u)q]\, f(\beta)\, d\beta, \end{aligned} \tag{24}$$

where $\tilde{\beta}$ follows the lognormal distribution in Eq. 13. Because the CARA–lognormal combination lacks a closed form, we follow standard practice and apply the mean–variance certainty-equivalent approximation:

$$\mathbb{E}[\beta] = \exp\Big(\mu_\beta + \tfrac{1}{2}\sigma_\beta^2\Big), \qquad \mathrm{Var}(\beta) = \Big(\exp(\sigma_\beta^2) - 1\Big)\exp\Big(2\mu_\beta + \sigma_\beta^2\Big).$$

Substituting these moments yields the certainty-equivalent function:

$$\begin{aligned} V(e_u, A_u) = \delta e_u q + (\Delta - A_u)\,&\frac{(A_u - B - C_{rm} + \theta e_u)\, v^2 q^2 \mathcal{M}^2}{k} - \frac{d}{2}\,e_u^2 \\ &+ (h_{ts}+\lambda e_u) q \mu_\beta - \frac{\gamma}{2}\Big[(h_{ts}+\lambda e_u)q\Big]^2 \sigma_\beta^2. \end{aligned} \tag{25}$$

From a business strategy perspective, risk aversion captures firms' preference for resilient, predictable circular supply chains. Higher uncertainty in secondary-material markets reduces willingness to invest upfront in eco-design, weakening the internal alignment that closed-loop systems otherwise create.

Lemma 3. *The optimal eco-design effort e_u^* and buy-back price A_u^* for a risk-averse manufacturer satisfy:*

$$e_u^* = \frac{q\left[-A_u^*\,\theta\,v^2\,q\,\mathcal{M}^2 + \Delta\,\theta\,v^2\,q\,\mathcal{M}^2 + \delta\,k - \gamma\,h_{ts}\,k\,\lambda\,q\,\sigma_\beta^2 + k\,\lambda\,\mu_\beta\right]}{k\left(d + \gamma\,\lambda^2\,q^2\,\sigma_\beta^2\right)}, \quad (26)$$

$$A_u^* = \frac{\Delta + B + C_{rm} - \theta e_u^*}{2}. \quad (27)$$

Proof. The proof of Lemma 3 is provided in the Appendix.

Equation 26 shows that both risk aversion (γ) and price volatility (σ_β^2) reduce the incentive to invest in eco-design: uncertainty increases the perceived cost of future returns, dampening the effectiveness of performance-oriented subsidy schemes. Equation 27 implies that lower effort also reduces the buy-back price, transmitting risk aversion downstream to recycling decisions.

Proposition 2. *The equilibrium of the closed-loop system with a risk-averse manufacturer and risk-neutral recycler is:*

1. *Buy-back price:*

$$A_u^{**} = \frac{k\left(d + \gamma\lambda^2q^2\sigma_\beta^2\right)(\Delta + B + C_{rm}) - \theta q\left[\Delta\,\theta v^2 q\mathcal{M}^2 + \delta k - \gamma\,h_{ts}k\lambda q\sigma_\beta^2 + k\lambda\mu_\beta\right]}{2k\left(d + \gamma\lambda^2q^2\sigma_\beta^2\right) - \theta^2v^2q^2\mathcal{M}^2}. \quad (28)$$

2. *Eco-design level:*

$$e_u^{**} = \frac{q\left[(B + C_{rm} - \Delta)\,\theta\,v^2\,q\,\mathcal{M}^2 - 2\delta k + 2\gamma\,h_{ts}k\lambda q\sigma_\beta^2 - 2k\lambda\mu_\beta\right]}{\mathcal{M}^2q^2\theta^2v^2 - 2k\left(d + \gamma\lambda^2q^2\sigma_\beta^2\right)}. \quad (29)$$

3. *Recycling rate:*

$$\rho_u^{**} = \frac{(A_u^{**} - B - C_{rm} + \theta e_u^{**})\,vq\mathcal{M}}{k}. \quad (30)$$

Risk aversion reduces all three decision variables, e_u^{**}, A_u^{**} and ρ_u^{**}, relative to the risk-neutral benchmark. The term $\gamma\sigma_\beta^2$ depresses eco-design incentives, and the resulting lower buy-back price suppresses recycling effort. Subsidy schemes calibrated for risk-neutral firms will therefore underperform when manufacturers seek stability, especially for capital-intensive recycling methods such as solvolysis (M2). Under Extended Producer Responsibility regimes, this implies that performance-based subsidies must account for risk preferences if they are to maintain closed-loop alignment.

4.1. Numerical Analysis of Subsidy Impact: Risk-Averse Case

Risk aversion affects circularity outcomes through two channels. First, it shifts decisions toward safer outcomes, lowering both e_{u,M_i}^{**} and A_{u,M_i}^{**} relative to the risk-neutral benchmark. Second, it reduces the marginal return to eco-design because the risky component of revenue, $\tilde{\beta}(h_{ts}+\lambda e_{u,M_i}^{**})q$, is discounted in the certainty equivalent. As a result, the marginal payoff of e_{u,M_i}^{**} declines even before cost convexities bind. Early design improvements remain essential to meet qualification and certification requirements (e.g. material testing thresholds in DNV GL AS (2015)) and to maintain fibre quality (Thomason et al., 2016). Beyond these thresholds, however, additional gains become harder to monetise, as procurement tends to prioritise price and availability over incremental performance improvements.

To ensure physical and institutional realism, we constrain the recycling rate to $\rho \in [\rho_{0,M_i}, 1]$, where ρ_{0,M_i} is the empirically observed baseline for each method and 1 denotes full circularity. We calibrate the subsidy in the risk-neutral case such that full circularity is achieved at a reference volatility $\sigma_\beta = 1$. This value, $\delta = \delta_{u,M_i}^{100\%}(\sigma_\beta{=}1)$, is indicated by a vertical dashed line in Figures 5a–5b. For $\sigma_\beta < 1$, the risk-neutral recycling rate lies below full circularity; for $\sigma_\beta > 1$, the risk-neutral interior solution would exceed 1, but the upper bound binds and the curve is flat at 1. Risk-averse outcomes are computed for $\gamma \in \{5 \times 10^{-6}, 1.0 \times 10^{-6}, 1.5 \times 10^{-6}\}$ and are floored at ρ_{0,M_i}, reflecting minimum-compliance or contractual obligations that prevent falling below existing practice.

Figures 5a and 5b show that, holding technology and costs fixed, increasing volatility σ_β depresses the recycling rate under risk aversion, $\rho^{**}_{u,M_i}(\gamma, \sigma_\beta)$, with larger effects at higher γ. The vertical dashed line marks $\sigma_\beta = 1$, where the risk-neutral benchmark reaches $\rho = 1$, corresponding to the EU's targets of eliminating blade landfill and achieving full recyclability (European Commission, 2020b, 2019; WindEurope, 2020).

Our calibration at $\sigma_\beta = 1$ therefore serves as a neutral benchmark. For $\sigma_\beta > 1$, the risk-neutral manufacturer continues to achieve full circularity (the curve remains capped at $\rho = 1$), whereas the risk-averse curves decline as σ_β increases. This decline reflects the additional subsidy required to compensate for the negative effect of uncertainty.

Table 6 quantifies this effect: the minimum subsidy required for full circularity, $\delta^{100\%}_{u,M_i}$, increases with both risk aversion γ and volatility σ_β. The increases are largest for capital-intensive or variance-sensitive methods such as M2, indicating that identical volatility shocks generate systemically different fiscal burdens across recycling technologies.

Our calibration at $\sigma_\beta = 1$ therefore provides a neutral reference: the risk-neutral curve is capped at full circularity for $\sigma_\beta > 1$, while risk-averse curves decline with σ_β, capturing the additional subsidy burden attributable

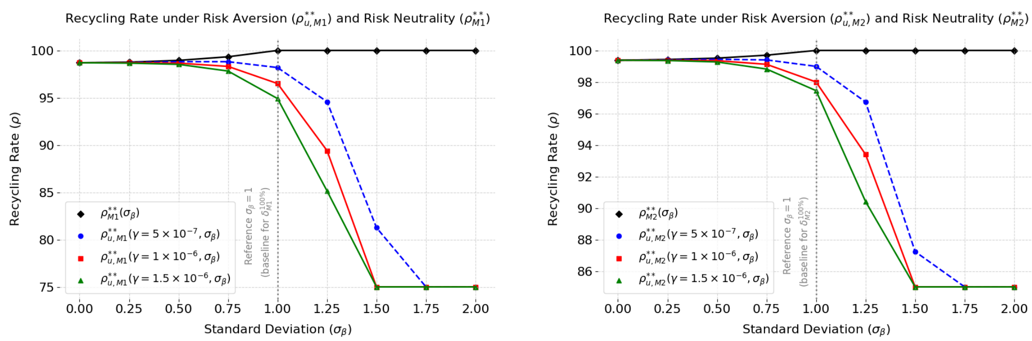

(a) Method 1: Pyrolysis

(b) Method 2: Solvolysis

Figure 5: Recycling rate under risk neutrality and risk aversion by volatility. The vertical dashed line marks $\sigma_\beta = 1$, where the risk-neutral system attains full circularity. Risk-neutral curves are capped at $\rho = 1$ for $\sigma_\beta > 1$; risk-averse curves are floored at ρ_{0,M_i}.

to uncertainty.

When fluctuations in the price and quality of recycled materials strongly influence investment decisions, relying on subsidies alone may not be the most cost-effective way to achieve circularity targets. In such settings, combining fiscal support with risk-management and technology policies can substantially improve outcomes.

First, instruments to reduce risk, such as quality-assurance standards, certification schemes, warranties, or insurance, reduce the uncertainty faced by manufacturers (i.e., lower σ_β or perceived risk captured by γ) (e.g., OECD, 2023; European Commission, 2020a). By making future prices and material performance more predictable, these instruments reduce the level of subsidy required for firms to invest in circular solutions.

Second, innovation and coordination policies, such as R&D support, eco-design standards, and long-term procurement commitments, raise the expected closed-loop value of materials (Δ) and either reduce recycler-side re-

Table 6: Subsidy coefficient $\delta_{u,M_i}^{100\%}$ required to achieve full recyclability under risk neutrality and risk aversion.

		$\delta_{M1}^{100\%}$	$\delta_{M2}^{100\%}$
Risk Neutrality	$\rho_{M_i}^{**}(\sigma_\beta) = 100\%$ $(\sigma_\beta = 1)$	1020	1330
		$\delta_{u,M1}^{100\%}$	$\delta_{u,M2}^{100\%}$
Risk Aversion	$(\gamma = 5 \times 10^{-6},\ \sigma_\beta = 1)$	1098	1425
	$(\gamma = 1.0 \times 10^{-6},\ \sigma_\beta = 1)$	1170	1500
	$(\gamma = 1.5 \times 10^{-6},\ \sigma_\beta = 1)$	1250	1592

cycling costs (C_{rm}) or increase eco-design leverage (θ), thereby improving the economic attractiveness of recycling technologies.

These interventions strengthen expected returns while also improving reliability (e.g., WindEurope, 2020).

These measures make circularity investments more resilient to market volatility and reduces the overall fiscal burden needed to meet policy targets.

Risk aversion weakens circular incentives by reducing manufacturers' willingness to invest in eco-design under uncertain future revenues. Even when subsidies are calibrated to achieve full circularity under risk neutrality, price volatility leads risk-averse firms to lower eco-design effort and buy-back prices, reducing recycling rates. As a result, subsidy schemes that ignore risk preferences systematically underestimate the fiscal support required to stabilise circular systems.

5. Risk Aversion and Competitive Leakage in a Closed-Loop System

We now extend the analysis to a more realistic setting in which recyclers may divert recovered material to higher-value external markets and resale prices are volatile. From a business strategy perspective, risk aversion reflects firms' preference for stable and resilient circular supply chains: volatility in secondary-material markets can disrupt investment, coordination, and long-term value capture. Competitive leakage therefore represents not only an economic friction, but a strategic threat to the stability of closed-loop coordination. When recyclers face more profitable external buyers, the closed-loop system loses material, undermining the manufacturer's circular business model and weakening incentives for eco-design.

Throughout this section, we treat the eco-design effort (e_u^{**}) and the buy-back price (A_u^{**}) as fixed at the risk-averse closed-loop values calibrated in Section 4. These values were obtained under the assumption of no leakage and represent the combination of (e, A) that delivers full circularity ($\rho = 1$) at the baseline subsidy level $\delta_u^{100\%}$, corresponding to the EU's target of full blade recyclability. In other words, e_u^{**} and A_u^{**} define the risk-averse manufacturer's optimal closed-loop strategy before the introduction of competitive leakage.

This modelling choice reflects well-documented technological and contractual lock-ins in composite-intensive industries. In wind energy, for example, the design of Vestas's CETEC platform and Siemens Gamesa's RecyclableBlade was finalised several years before product launch. Resin systems, fibre architectures, and joint geometries were fixed early to secure certification and supplier integration, making mid-production design changes costly and disruptive (Ulrich and Eppinger, 2015; Luttropp and Lagerstedt, 2006). Similar rigidities arise in aerospace and marine applications, where multi-year recycling contracts pre-define quality, delivery, and pricing requirements to ensure traceability and regulatory compliance (Cachon and Lariviere, 2005).

In such settings, policy commonly operates ex post. Once blade designs are locked and suppliers are contracted, manufacturers cannot readily re-optimise eco-design decisions. Consistent with this reality, our model does not re-optimise manufacturer behaviour. Instead, we compute the incremental subsidy $\delta_u^{\min}$ required to retain recovered material within the closed-loop when recyclers face competitive external resale opportunities. The total policy requirement is therefore

$$\delta_u^{\text{total}} = \delta_u^{100\%} + \delta_u^{\min},$$

where $\delta_u^{100\%}$ is the subsidy needed to reach full circularity under locked-in design choices, and $\delta_u^{\min}$ is the additional amount required to prevent leakage of recovered fibres to external markets.

Leakage occurs when the manufacturer's effective buy-back value is below the external resale price. Let $\tilde{A}_C$ denote the random external market price, and let θe_u^{**} represent the per-ton cost reduction induced by the manufacturer's eco-design effort. Consistent with segmented secondary markets, we assume that $\tilde{A}_C$ is independent of (A_u^{**}, e_u^{**}). The recycler sells to the manufacturer only if

$$A_u^{**} + \theta e_u^{**} \;\geq\; \tilde{A}_C.$$

Following evidence from secondary-material markets—where prices are volatile, right-skewed, and strictly positive—we assume $\tilde{A}_C \sim \text{LN}(\mu_C, \sigma_C^2)$ (European Environment Agency, 2023; U.S. EPA, 2020; Lee et al., 2019), with density

$$f_{\tilde{A}_C}(A_C) = \frac{1}{A_C \sigma_C \sqrt{2\pi}} \exp\left[-\frac{(\ln A_C - \mu_C)^2}{2\sigma_C^2}\right], \quad A_C > 0.$$

To ensure that recovered material is retained with at least probability α, the following condition must hold:

$$\Pr(\tilde{A}_C \leq A_u^{**} + \theta e_u^{**}) \geq \alpha.$$

For the log-normal distribution, this is equivalent to

$$\Phi\left(\frac{\ln(A_u^{**} + \theta e_u^{**}) - \mu_C}{\sigma_C}\right) \geq \alpha.$$

Defining the robustness-adjusted external price (the α-quantile) as

$$A_C^{\alpha} = \exp\Big(\mu_C + \Phi^{-1}(\alpha)\sigma_C\Big),$$

the closed-loop condition becomes

$$A_u^{**} + \theta e_u^{**} \;\geq\; A_C^{\alpha}.$$

Here, A_C^{α} is the robustness-adjusted threshold that must be matched for the loop to remain stable despite volatility and leakage pressure.

A per-unit-of-effort subsidy to the manufacturer, $S(e) = \delta e q$, increases the recycler-relevant €/t offer by $\phi\, \delta e/(v\mathcal{M})$, where $\phi \in [0, 1]$ is the pass-through rate, converting a per-blade subsidy to its €/t equivalent (each blade yields $v\mathcal{M}$ tonnes of recovered material). Setting $\phi = 1$ in the baseline, the loop-closure condition becomes

$$A_u^{**} + \theta e_u^{**} + \frac{\delta\, e_u^{**}}{v\mathcal{M}} \;\geq\; A_C^{\alpha}.$$

Solving for the minimum incremental subsidy and enforcing non-negativity yields, for $e_u^{**} > 0$,

$$\delta_u^{\min} = \frac{v\,\mathcal{M}}{e_u^{**}}\left[A_C^{\alpha} - A_u^{**} - \theta e_u^{**}\right]^{+}, \tag{31}$$

where $[x]^{+} = \max\{0, x\}$ ensures $\delta^{\min} = 0$ whenever the manufacturer's offer already exceeds the robustness-adjusted threshold. Note that the subsidy does not alter eco-design effort ex post, as e_{u,M_i}^{**} is fixed by technological and contractual lock-ins. Instead, the subsidy effectively raises the manufacturer's €/t offer to the recycler, via the pass-through mechanism in $S(e)$, ensuring retention without re-optimising upstream decisions.

The expression is well defined for $e_u^{**} > 0$; if $e_u^{**} = 0$, retention cannot be enforced through $S(e)$ alone and would require either a higher buy-back price A_u^{**} or a lump-sum top-up instrument.

Equation (31) also yields intuitive comparative statics. First, the incremental subsidy is increasing in both external price volatility and the robustness requirement, i.e. $\partial\delta^{\min}/\partial\sigma_C > 0$ and $\partial\delta^{\min}/\partial\alpha > 0$, so greater market uncertainty or stricter retention targets raise the required premium to keep material in the loop. Second, higher buy-back commitments A_u^{**}, stronger eco-design leverage θ, and greater effort e_u^{**} all reduce $\delta^{\min}$, since they raise the effective value of the circular-chain offer relative to external resale opportunities.

In strategic terms, leakage risks amplify the fiscal burden of sustaining circularity and weaken incentive alignment across the value chain. Closed-loop business models thus require not only economic incentives but also governance mechanisms that stabilise material flows under uncertainty.

5.1. Numerical Illustration under Risk Aversion: Impact of Leakage on Subsidy Needs

This subsection operationalises the leakage model to quantify the additional fiscal effort required to sustain circularity under market competition. The risk-averse closed-loop pair $(e^{**}_{u,M_i}, A^{**}_{u,M_i})$ is held fixed at the subsidy level that attains full circularity in the no-leakage setting (Section 4), adopting a benchmark risk-aversion coefficient of $\gamma = 1.0 \times 10^{-6}$. We then compute the incremental subsidy $\delta^{\min}_{u,M_i}$ required to keep recovered fibre within the loop when recyclers face profitable external resale opportunities.

The incremental subsidy is evaluated using Equation (31) as a function of (i) the target retention probability α and (ii) the volatility of external resale prices σ_C. This isolates the effect of competitive leakage and market risk without re-optimising manufacturer behaviour. All subsidy values are reported in euros per blade per unit of eco-design effort, consistent with $S(e) = \delta eq$; conversion to euros per tonne follows by dividing by $v\mathcal{M}$. The total subsidy under leakage is therefore

$$\delta^{\text{total}}_{u,M_i} = \delta^{100\%}_{u,M_i} + \delta^{\min}_{u,M_i}.$$

External resale prices are assumed lognormally distributed, $\tilde{A}_C \sim \text{LN}(\mu_C, \sigma_C^2)$, with μ_C calibrated to a target mean $\bar{A}_C$ via $\mu_C = \ln(\bar{A}_C) - \frac{1}{2}\sigma_C^2$, ensuring $\mathbb{E}[\tilde{A}_C] = \bar{A}_C$. We set $\bar{A}_C = 2000$ €/t and 3000 €/t for M1 and M2, respectively, reflecting plausible differences in resale value for lower- and higher-grade recovered fibres. These levels are consistent with the equilibrium buy-back price ranges obtained in the risk-averse calibration. We explore robustness targets $\alpha \in [0.50, 0.95]$ and volatility levels $\sigma_C \in [0.2, 1.4]$.

Table 7 reports the incremental subsidy as α varies at fixed $\sigma_C = 1$. The additional subsidy remains small for moderate robustness requirements but rises sharply as $\alpha \to 1$. Achieving 95% retention requires roughly five times the support needed for 50%, since the robustness threshold A_C^{α} shifts deep into the heavy right tail of the lognormal distribution, making the manufacturer's offer increasingly difficult to match.

Table 7: Incremental ($\delta_{u,M_i}^{\min}$) and total ($\delta_{u,M_i}^{\text{total}}$) subsidy requirements as a function of robustness target α at fixed market volatility $\sigma_C = 1$.

Robustness α	0.50	0.60	0.70	0.80	0.85	0.90	0.95
$\delta_{u,M_1}^{\min}$	0.00	0.00	0.00	0.00	6.59	124.41	392.07
$\delta_{u,M_1}^{\text{total}}$	1170.00	1170.00	1170.00	1170.00	1176.59	1294.41	1562.07
$\delta_{u,M_2}^{\min}$	0.00	0.00	0.29	100.52	230.28	434.66	852.45
$\delta_{u,M_2}^{\text{total}}$	1500.00	1500.00	1500.29	1600.52	1730.28	1934.66	2352.45

Table 8 fixes $\alpha = 0.90$ and varies σ_C. As volatility increases, the incremental subsidy required to maintain loop closure rises, with strong sensitivity in high-variance regimes where the robustness-adjusted price A_C^{α} becomes difficult to match. M1 requires slightly less additional support than M2 because its buy-back value—augmented by eco-design cost savings—lies closer to external resale levels. This difference arises from calibrated relative price levels rather than technological advantages.

All values in Tables 7 and 8 are expressed in euros per blade per unit of eco-design effort, consistent with $S(e) = \delta_{u,M_i}^{\text{total}} e_{u,M_i}^{**} q$.

Figure 6 visualises these relationships. The 2020 EU Circular Economy

Table 8: Incremental ($\delta^{\min}_{u,M_i}$) and total ($\delta^{\text{total}}_{u,M_i}$) subsidy requirements as a function of market volatility σ_C at fixed robustness target $\alpha = 0.90$.

Uncertainty σ_C	0.2	0.4	0.6	0.8	1.0	1.2	1.4
$\delta^{\min}_{u,M_1}$	0.00	7.33	40.54	78.69	113.38	136.15	146.98
$\delta^{\text{total}}_{u,M_1}$	1170.00	1177.33	1210.54	1248.69	1283.38	1306.15	1316.98
$\delta^{\min}_{u,M_2}$	35.06	117.74	196.64	264.20	314.89	343.29	346.38
$\delta^{\text{total}}_{u,M_2}$	1535.06	1617.74	1696.64	1764.20	1814.89	1843.29	1846.38

Action Plan emphasises the importance of design-for-reuse principles and stronger secondary markets (European Commission, 2020a). Our results refine this insight: when recyclers face profitable external buyers, the alignment between manufacturer incentives and circularity outcomes weakens. In such cases, shocks to robustness requirements or market volatility necessitate complementary governance instruments—such as standards, traceability systems, or long-term offtake contracts—in addition to subsidies, in order to maintain material retention at lower fiscal cost.

Leakage occurs when external resale markets offer higher and more volatile prices than the buy-back price offered by the manufacturer to keep materials in the closed loop. In such conditions, recyclers divert recovered materials away from the closed loop unless additional support compensates for this gap. The required subsidy increases sharply with market volatility and robustness targets, implying that subsidy-only approaches become increasingly inefficient when secondary markets are competitive and uncertain.

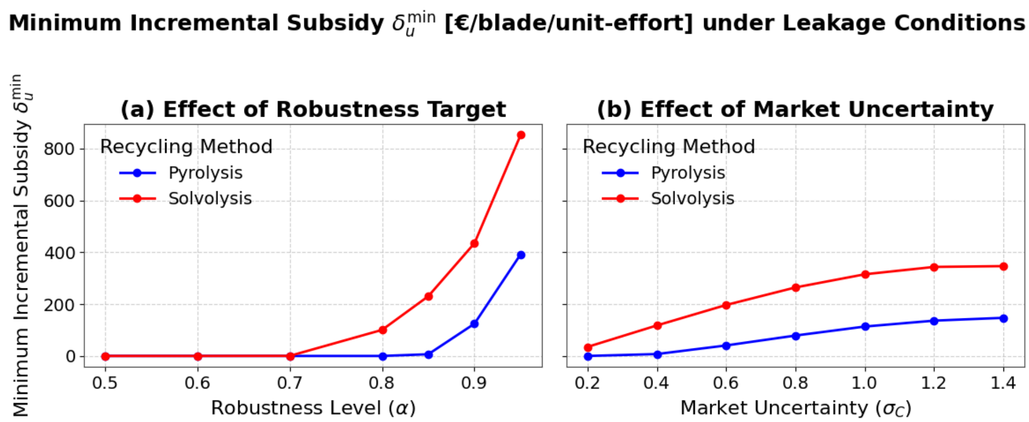

Figure 6: Minimum incremental subsidy ($\delta^{\min}$) under alternative leakage conditions. Panel (a) shows the effect of robustness level α; Panel (b) shows the effect of market uncertainty σ_C.

6. Conclusion and Policy Implications

This paper has examined the conditions under which closed-loop circularity can operate as a strategic and institutional coordination mechanism, aligning private incentives with societal objectives even when eco-design effort is hidden. In the Stackelberg framework developed here, the manufacturer's reliance on recycled inputs endogenously rewards eco-design through cost-reduction feedbacks, thereby reducing the need for explicit monitoring of upstream actions. However, this self-alignment is fragile. Risk aversion, revenue volatility, and competitive leakage systematically weaken the incentives that sustain circularity, underscoring the vulnerability of closed-loop systems in real-world market environments.

Our analysis shows that performance-based subsidies can effectively support circularity under hidden action, but only within limits. When external resale opportunities are attractive or price volatility is high, subsidy requirements rise sharply, especially for stringent robustness targets. Under these conditions, a subsidy-only approach becomes fiscally inefficient and may fail to secure long-term material retention. The results highlight that stability, rather than scale alone, is central to the durability of circular business models.

Policy design should therefore prioritise instruments that reduce uncertainty and strengthen commitment within the circular chain. Robustness-adjusted, incremental subsidies can address short-run leakage risks, but they must be complemented with de-risking mechanisms such as long-term offtake agreements, advance-purchase commitments, price floors, insurance products, and minimum-retention clauses. Standards, certification schemes, and traceability systems can further enhance the intrinsic value of recycled inputs by strengthening eco-design leverage and embedding incentive alignment within market and regulatory structures.

Closed-loop stability should be recognised as a policy objective in its own right. Broader regulatory tools—including landfill restrictions, carbon pricing, extended producer responsibility, and green public procurement—can reinforce circularity while reducing long-run fiscal exposure. By formalising how uncertainty, leakage, and hidden action interact, this paper provides a foundation for designing policy mixes that stabilise circular value chains under risk.

The analysis focuses on a simplified setting with one manufacturer and one recycler and does not model strategic competition among multiple firms or more complex policy instruments. This simplification allows the model to highlight the core governance mechanisms underlying circular coordination, while still capturing competitive pressures through leakage to external markets. Future research could extend the model to dynamic technology learning, cross-sector material flows, and intertemporal investment decisions, where feedback loops and path dependence shape long-run outcomes. The framework is applicable to other composite-intensive sectors, such as aerospace, marine, and construction, where eco-design is difficult to observe and volatility in secondary markets constrains the emergence of robust circular economies.

Declaration of Conflict of Interest

The authors declare that they have no known competing financial interests or personal relationships that could have appeared to influence the work reported in this paper.

References

Agrawal, S., Kumar, D., Singh, R.K., Singh, R.K., 2023. Analyzing coordination strategy of circular supply chain in re-commerce industry: A game theoretic approach. Business Strategy and the Environment 32. doi:10.1002/bse.3152.

Åkesson, D., Foltynowicz, Z., Christeen, J., Skrifvars, M., 2012. Microwave pyrolysis as a method of recycling glass fibre from used blades of wind turbines. Journal of Reinforced Plastics and Composites 31, 1136–1142. doi:10.1177/0731684412453512.

Altenburg, T., Engelmeier, T., 2013. Boosting solar investment with limited subsidies: Rent management and policy learning in india. Energy Policy

59, 866–874. URL: https://doi.org/10.1016/j.enpol.2013.04.055, doi:10.1016/j.enpol.2013.04.055.

Aryee, R., 2025. Theories and theoretical approaches in circular economy research. Business Strategy and the Environment doi:10.1002/bse.70343.

Beauson, J., 2022. End-of-life of wind turbine blades – Value chain, recycling and composite materials. Technical Report. Technical University of Denmark, DTU Wind Energy, Risø Campus. Roskilde, Denmark. doi:10.11581/DTU.00000221.

Bimonte, G., Ioppolo, G., Senatore, L., Trincone, B., 2022. Government eco-innovation incentives in a recycling system: A stackelberg-type model. Business Strategy and the Environment doi:10.1002/bse.3337.

Bocken, N.M.P., Short, S.W., Rana, P., Evans, S., 2014. A literature and practice review to develop sustainable business model archetypes. Journal of Cleaner Production 65, 42–56. doi:10.1016/j.jclepro.2013.11.039.

Boukhatmi, , Van Opstal, W., 2025. How can digital platforms resolve market failures to foster a circular economy? Business Strategy and the Environment doi:doi.org/10.1002/bse.70190.

Cachon, G.P., Lariviere, M.A., 2005. Supply chain coordination with revenue-sharing contracts: Strengths and limitations. Management Science 51, 30–44. doi:https://doi.org/10.1287/mnsc.1040.0215.

Calel, R., Colmer, J., Dechezleprêtre, A., Glachant, M., 2025. Do carbon offsets offset carbon? American Economic Journal: Applied Economics

17, 1–40. URL: https://doi.org/10.1257/app.20230052, doi:10.1257/app.20230052.

Chen, J., Wang, J., Ni, A., 2019. Recycling and reuse of composite materials for wind turbine blades: An overview. Journal of Reinforced Plastics and Composites 38, 567–577. doi:10.1177/0731684419833470.

DNV GL AS, 2015. Dnvgl-st-0376: Rotor blades for wind turbines. Edition December 2015. Available at: https://studylib.net/doc/18232146/dnvgl-st-0376-rotor-blades-for-wind-turbines.

Enciso-Alfaro, S., García-Sánchez, I., 2025. Circular economy: A pathway to integrated value creation for business and society. Business Strategy and the Environment doi:10.1002/bse.70255.

European Commission, 2008. Directive 2008/98/ec of the european parliament and of the council on waste and repealing certain directives (waste framework directive). https://eur-lex.europa.eu/legal-content/EN/TXT/?uri=CELEX:32008L0098.

European Commission, 2019. The European Green Deal (COM/2019/640 final). Technical Report. European Commission. URL: https://eur-lex.europa.eu/legal-content/en/ALL/?uri=CELEX:52019DC0640. accessed: August 4, 2025.

European Commission, 2020a. A new circular economy action plan: For a cleaner and more competitive europe. URL: https://eur-lex.europa.eu/legal-content/EN/TXT/?uri=CELEX:52020DC0098. cOM(2020) 98 final, Brussels.

European Commission, 2020b. A New Circular Economy Action Plan: For a Cleaner and More Competitive Europe (COM/2020/98 final). Technical Report. European Commission. URL: https://eur-lex.europa.eu/legal-content/en/ALL/?uri=CELEX:52020DC0098. accessed: August 4, 2025.

European Environment Agency, 2023. Markets for many commonly recycled materials struggle in the eu. URL: https://www.eea.europa.eu/en/newsroom/news/markets-commonly-recycled-materials-struggle.

Ferrell, S.L., DeVuyst, E., 2013. Decommissioning wind energy projects: An economic and political analysis. Energy Policy 53, 105–113. doi:10.1016/J.ENPOL.2012.10.017.

Fonte, R., Xydis, G., 2021. Wind turbine blade recycling: An evaluation of the european market potential for recycled composite materials. Journal of Environmental Management 287, 112269. doi:10.1016/j.jenvman.2021.112269.

Gautam, D., Bolia, N., 2024. Developing an incentive-based model for efficient product recovery and reverse logistics. Business Strategy and the Environment 33. doi:10.1002/bse.3330.

Giorgini, L., Leonardi, C., Mazzocchetti, L., Zattini, G., Cavazzoni, M., Montanari, I., Tosi, C., Benelli, T., 2016. Pyrolysis of fiberglass/polyester composites: Recovery and characterization of obtained products. FME Transactions 44, 405–414. doi:10.5937/FMET1604405G.

de Gorter, H., Drabik, D., Just, D.R., 2013. The economics of a blend mandate for biofuels. American Journal of Agricultural Economics 95, 738–750. doi:doi.org/10.1111/j.1467-8276.2009.01275.x.

Korhonen, J., Honkasalo, A., Seppälä, J., 2018. Circular economy: The concept and its limitations. Ecological Economics 143, 37–46. doi:doi.org/10.1016/j.ecolecon.2017.06.041.

Lee, C.F., Lee, J.C., Lee, A.C., 2019. Normal, lognormal distribution and option pricing model, in: Handbook of Quantitative Finance and Risk Management. Springer, pp. 421–428. URL: https://link.springer.com/chapter/10.1007/978-0-387-77117-5_27.

Liu, P., Meng, F., Barlow, C.Y., 2022. Wind turbine blade end-of-life options: An economic comparison. Resources, Conservation and Recycling 180, 106202. doi:doi.org/10.1016/j.resconrec.2022.106202.

Lund, K., Madsen, E., 2024. State-of-the-art value chain roadmap for sustainable end-of-life wind turbine blades. Renewable and Sustainable Energy Reviews 192, 114234. doi:doi.org/10.1016/j.rser.2023.114234.

Luttropp, C., Lagerstedt, J., 2006. Ecodesign and the ten golden rules: Generic advice for merging environmental aspects into product development. Journal of Cleaner Production 14, 1396–1408. doi:doi.org/10.1016/j.jclepro.2005.11.022doi=.

Martinez Leal, J., Pompidou, S., Charbuillet, C., Perry, N., 2020. Design for and from recycling: A circular ecodesign approach to improve the circular economy. Sustainability 12, 9861. URL: https://doi.org/10.3390/su12239861, doi:10.3390/su12239861.

McKinsey & Company, 2023. Renewable-energy development: Disrupted supply chains. McKinsey Insight. URL: https://www.mckinsey.com/industries/electric-power-and-natural-gas/our-insights/renewable-energy-development-in-a-net-zero-world-disrupted-supply-chains.

OECD, 2016. Extended Producer Responsibility: Updated Guidance for Efficient Waste Management. Organisation for Economic Co-operation and Development, Paris. doi:10.1787/9789264256385-en.

OECD, 2023. Financing the circular economy. URL: https://www.oecd.org/environment/financing-the-circular-economy.htm. oECD Environment Policy Paper No. 33.

Oliveux, G., Dandy, L.O., Leeke, G.A., 2015. Current status of recycling of fibre reinforced polymers: Review of technologies, reuse and resulting properties. Progress in Materials Science 72, 61–99. doi:10.1016/j.pmatsci.2015.01.004.

Pender, K., Romoli, F., Fuller, J., 2024. Lifecycle assessment of strategies for decarbonising wind blade recycling toward net zero 2050. Energies 17, 3008. doi:10.3390/en17123008.

Rahman, S.u., Shakeel, S.R., 2025. Challenges in renewable energy supply chains: Strategies for a sustainable energy future, in: Gandomi, M., Ahmadi, A., et al. (Eds.), Sustainable Supply Chain of Renewable Energy Networks. Springer, pp. 125–144. doi:10.1007/978-981-96-4940-2_6.

Rosa, A.D.L., Greco, S., Tosto, C., Cicala, G., 2021. LCA and LCC of a chemical recycling process of waste CF-thermoset composites for the production of novel CF-thermoplastic composites. open loop and closed loop scenarios. Journal of Cleaner Production 320, 127158. doi:10.1016/j.jclepro.2021.127158.

Sardana, S., Singh, V., Adhikari, D.R., 2024. Sustainable product design, in: Advances in E-Business Research Series. IGI Global, pp. 65–90. doi:10.4018/979-8-3693-9699-5.ch004.

Siemens Gamesa Renewable Energy, 2021. Siemens gamesa launches world's first recyclable wind turbine blade for commercial use. https://www.siemensgamesa.com/en-int/newsroom/2021/09/210908-siemens-gamesa-launches-world-first-recyclable-wind-turbine-blade. Accessed: 2025-08-03.

Sokoli, H.U., Beauson, J., Simonsen, M.E., Fraisse, A., Brøndsted, P., Søgaard, E.G., 2017. Optimized process for recovery of glass- and carbon fibers with retained mechanical properties by means of near- and supercritical fluids. The Journal of Supercritical Fluids 124, 80–89. doi:10.1016/j.supflu.2017.01.013.

Sproul, E., Williams, M., Rencheck, M., Korey, M., Ennis, B., 2023. Life cycle assessment of wind turbine blade recycling approaches in the united states. IOP Conference Series: Materials Science and Engineering 1293, 012027. doi:10.1088/1757-899X/1293/1/012027.

Stahel, W.R., 2016. The circular economy. Nature 531, 435–438. doi:10.1038/531435a.

Szatkowski, P., Twaróg, R., 2024. Thermal recycling process of carbon fibers from composite scrap—characterization of pyrolysis conditions and determination of the quality of recovered fibers. Fibers 12, 68. doi:10.3390/fib12080068.

Tapper, R.J., Longana, M.L., Yu, H., Hamerton, I., Potter, K.D., 2018. Development of a closed-loop recycling process for discontinuous carbon fibre polypropylene composites. Composites Part B: Engineering 146, 222–231. doi:10.1016/j.compositesb.2018.03.048.

Thapa, M., Missoum, S., 2022. Surrogate-based stochastic optimization of horizontal-axis wind turbine composite blades. Structural and Multidisciplinary Optimization 65, Article 41. doi:10.1007/s00158-021-03114-8.

Thomason, J.L., Jenkins, P., Yang, L., 2016. Glass fibre strength: A review with relation to composite recycling. Fibers 4, 18. doi:10.3390/fib4020018.

Ulrich, K.T., Eppinger, S.D., 2015. Product Design and Development. 6th ed., McGraw-Hill Education.

U.S. EPA, 2020. Historical recycled commodity values. URL: https://www.epa.gov/sites/production/files/2020-07/documents/historical_commodity_values_07-07-20_fnl_508.pdf.

Vestas Wind Systems A/S, 2023. Sustainability report 2022. Retrieved

August 3, 2025, from https://www.vestas.com/en/sustainability/reports-and-ratings.

WindEurope, 2020. How to build a circular economy for wind turbine blades through policy and partnerships. URL: https://windeurope.org/intelligence-platform/product/how-to-build-a-circular-economy-for-wind-turbine-blades-through-policy-and-part retrieved 2024-02-07.

WindEurope, 2023. Blade recycling a top priority for the wind industry. https://windeurope.org/newsroom/news/blade-recycling-a-top-priority-for-the-wind-industry/. Accessed 11 Aug 2025.

Yazan, D.M., Yazdanpanah, V., Fraccascia, L., 2020. Learning strategic cooperative behavior in industrial symbiosis: A game-theoretic approach integrated with agent-based simulation. Business Strategy and the Environment doi:10.1002/bse.2488. first published: 03 March 2020.

Yu, H., Chang, X., Liu, W., 2021. Cost-based subsidy and performance-based subsidy in a manufacturing-recycling system considering product eco-design. Journal of Cleaner Production 327, 129391. doi:10.1016/j.jclepro.2021.129391.

Zabihi, O., Ahmadi, M., Liu, C., Mahmoodi, R., Li, Q., Ghandehari Ferdowsi, M.R., Naebe, M., 2020. A sustainable approach to the low-cost recycling of waste glass fibres composites towards circular economy. Sustainability 12, 641. doi:10.3390/su12020641.

Zhao, Y., Wang, M., Lin, J., Liu, W., Chen, L., Wang, Z., Sun, B., Li, X., 2024. Exploring recycling strategies for retired wind turbine blades: The impact of policy subsidies and technological investments using a game-theoretic approach. Journal of Cleaner Production doi:10.1016/j.jclepro.2024.144628.